X-692-70-431
PREPRINT

THE MAGNETIC FIELD GEOMETRY OF JUPITER AND ITS RELATION TO IO MODULATED JOVIAN DECAMETRIC RADIO EMISSION

KENNETH H. SCHATTEN
NORMAN F. NESS

AUGUST 1970

GSFC
GODDARD SPACE FLIGHT CENTER
GREENBELT, MARYLAND

X-692-70-431

THE MAGNETIC FIELD GEOMETRY OF JUPITER AND ITS RELATION TO IO MODULATED JOVIAN DECAMETRIC RADIO EMISSION

Kenneth H. Schatten
Norman F. Ness*

Laboratory for Extraterrestrial Physics
NASA-Goddard Space Flight Center
Greenbelt, Maryland 20771

August 1970

*On leave at the University of Rome, Roma, Italy

Abstract

Observations of the Io modulated Jovian decametric radio emission have been compared with calculations of the magnetic field line passing through Io. Calculations of the angle between the earth and the magnetic field line near Io and both the northern and southern foot points of that field line with the surface of the planet were undertaken. Four emission sources favorable for synchrotron emission were located by presuming the earth-north (or south) threaded field intersection angle was near 90 degrees and the declination of Io was positive. These four sources correspond closely to the three major observed emission regions and to one infrequently observed.

These calculations imply little distortion of the Jovian magnetic field by Io. This assumption is quite reasonable as the moon, an object similar in size and density to Io, produces little effect upon the interplanetary magnetic field. A mechanism by which Io could stimulate the emission is presented that is consistent with the calculations conducted.

Introduction

An excellent account of the discovery by Burke and Franklin (1955) of Jovian associated radio emission is presented by Smith (1969) in a review article on the subject of Jupiter's radio emission. Bigg (1964) showed that Io, the innermost of Jupiter's four large moons, affected the Jovian decametric radio emission. Figure 1 from Dulk (1965) is an observed joint probability distribution for decametric radio emission from Jupiter as a function of the longitude of Jupiter, LCM, and the position or phase of Io, ϕ_{Io}. The source labeled A is often referred to as the Main source, B as the Early source, and C as the Third source. A fourth source has been suggested by Dulk (1965; and Warwick (1967) but, as he points out emission in this region is recorded infrequently so that it does not show as a separate source on the histograms. Dulk confines this source to a narrow range of Io's position centered at 100° and a 90° range of Jupiter's longitude centered at about 45°. This source is only seen at low frequencies and thus only when the earth's ionosphere is very quiet.

An extensive study of Jupiter's decametric emission by Warwick (1963) suggested to him that the magnetic field of Jupiter could be represented by the field resulting from a tilted off-center dipole. This dipole was tilted 9° with respect to Jupiter's rotational axis and directed towards a system III longitude of 200°. In a cartesian system (X, Y, Z), with the Z axis in the direction of rotation and the X-axis located along λIII = 200°, and the Y-axis chosen to establish a right-handed coordinate system, the coordinates of the Warwick dipole model would be (0.15, 1.11, -0.73) in Jovian radii. This dipole model was established from observations of the decametric

radio emission and also was felt to be consistent with asymmetries present in the decimetric sources of radio emission.

At present it is not clear that a displaced dipole is even the best way of approximating the Jovian magnetic field. With little else to rely on, however, this paper will initially assume the tilted off-center dipole model for the Jovian magnetic field and later compare it with the centered dipole model with a tilt of 10° directed towards $\lambda_{III}=200^{\circ}$.

A number of authors have proposed rather interesting but complex models for the observed Io associated decametric radio emission. The reader is referred to the articles of Warwick (1968), Zheleznyakov (1965), Ellis (1965), Gledhill (1967), Piddington and Drake (1968), and Goldreich and Lynden-Bell (1969). The models proposed by these authors are summarized in Table I.

It is the purpose of this paper to present a method of testing models of the Io associated Jovian decametric radio emission. In addition, it is suggested that Io may be moonlike in its interaction with the Jovian environment. That is, it may not affect its magnetic environment with any large scale embedded magnetic field nor with any electrical conducting influence. This may lead to a region near Io containing particles with disturbed pitch angle distributions which are responsible for subsequent emission near the mirror points which are close to the Jovian surface.

Jovian Magnetosphere and Io Interaction

The observed physical characteristics of the moon and Io are listed in Table II. As can be seen, the two satellites have approximately the same gross characteristics. Without knowledge to the contrary, it is natural to suggest they behave electrically and magnetically similar. The electrical conductivity and magnetic properties of the moon as interpreted from Lunar Explorer 35 observations have been discussed by Ness (1970) and Behannon (1968).

The flow of the solar wind past the moon may be represented as that of a super-Alfvénic plasma flow past an inert spherical object. The situation is somewhat different between the Jovian magnetosphere and Io. As discussed by Marshall and Libby (1967), it is expected that a forward reaching plasma proboscis will be formed since the rotation of the Jovian magnetosphere carries plasma and field lines past Io at a relative velocity of about 60 k/sec. The top portion of Figure 2 shows this geometry.

If however, the Jovian magnetosphere does not rigidly rotate with the planet but is fixed in space, as might occur should a non-conducting surface exist between the planet and Io, the relative velocity would then be about 17 km/sec, as Dulk (1965) notes. The Alfvén velocity in the vicinity of Io's orbit assuming a plasma density of 10 ions/cm^3 would then be 5×10^4 km/sec which is one thousand times the relative velocity. Thus, it is probable that a sub-Alfvénic flow of the plasma exists near Io and the magnetic field of the plasma will appear to be swept through Io without distortion. See Figure 2 (bottom).

In either the super-Alfvénic flow situation or the sub-Alfvénic flow situation, the magnetic field sweeps through Io relatively undisturbed. Energetic electrons or ions in the plasma may, however, be greatly affected by Io. This will be discussed later.

Computer Simulation

We shall now investigate the possibility that synchrotron emission is produced either near Io or as a result of the dumping of energetic particles near Jupiter at either of the two footpoints of the field line passing through Io. The bulk of the emission is assumed to be directed in a plane perpendicular to the field line. Thus, to test the model, the angle between the earth and the magnetic field at these locations was calculated. A direct comparison of the calculated angles for the major sources of emission (angle $\sim 90^{\circ}$) can test the validity of different models.

This geometry is shown in Figure 3. The angles between the earth and the magnetic fields at Io, the north footpoint and the south footpoint have been calculated as a function of the longitude of Jupiter and the phase of Io throughout the years 1961-1964 to compare with Figure 1. Histograms of the average angles at function of LCM and ϕ_{Io} in 30° buckets are shown in Figures 4-9. Shaded areas represent angles close to 90 degrees to compare with the location of observed decametric radio bursts. Figure 4, 5 and 6 are histograms of these average angles utilizing the Warwick dipole model previously discussed. As can be seen, the three major emission sources do have earth-field line angles close to 90° in each of these figures.

Gulkis and Carr (1966) plotted the positions of the decametric radio emission sources as functions of zenocentric declination of the earth and the central meridian longitude of Jupiter in system III (1957.0) coordinates and found that the emission sources were restricted to either plus or minus 6° zenomagnetic latitude. This is an interesting result as it may relate to the aspect of the magnetic field line at the emission region to the Jovian magnetic axis. If the radio bursts are emitted near 90° from the magnetic field line, then from simple geometric considerations the field source must be directed $\pm 6^{\circ}$ from Jupiter's magnetic axis. It is important to note that the results of Gulkis and Carr are independent of whether or not the Jovian magnetic field is centered on the planet.

In the case of a pure dipole field geometry, the angle of the magnetic field direction from the dipole axis is 1.5 times the angle between the location of that region and the dipole axis for small angles. Thus the latitude of the emission region may be at $\pm 4^{\circ}$ from the magnetic axis of Jupiter. Figure 7 and 8 show the angle of the North (and South) footpoints to the magnetic axis. As can be seen the angle is almost constant as a function of both Io phase and Jovian longitude. This means that the footpoint is located at nearly constant zenocentric magnetic latitude. This implies that emission also occurs at roughly constant zenomagnetic latitude as observed by Gulkis and Carr. An angle of 4° might be suggested by their observations. The southern footpoint is closer to this position than the northern footpoint. This would suggest it to be the more likely candidate for the emitting region. The southern footpoint field angle seems also to fit the observations better than the other two cases.

Io Influence

A discussion now follows as to one possible mechanism that will enable a non-conducting, non-magnetic satellite to exert a large influence on its environment. Figure 2 shows two possible interactions of a non-conducting and non-magnetic satellite on its environment. In each of these cases electric fields parallel to the magnetic field may arise. The effects of this phenomena have been observed in the first case indirectly by Ness and Schatten (1969) as high frequency fluctuations in the magnetic field far from the lunar wake. These field fluctuations are thought to result from electrons reflected upstream by an electric field in the lunar wake. This electric field is necessary to repel the electrons from the lunar wake thus insuring charge neutrality of the wake plasma. These electrons in turn disturb the magnetic environment in the case of the moon by producing high frequency oscillations in the field external to the wake.

Parallel electric fields may also arise in the sub-Alfvenic case by the Langmuir effect developing a space charge around the satellite or by photoionization. Such effects could result in electrons being repelled from Io with different pitch angle distributions as in the lunar case. These electrons could initialize a decametric radio storm as they make their way toward their mirror locations nearer to the surface of the planet. Io, lying on the outer edge of the Jovian radiation belt, might be in a favored position to reflect electrons to the southern footpoint if it were at a northern zenomagnetic latitude. Figure 9 shows the magnetic declination of Io computed as before.

It is now assumed that the probability of observing decametric radio emission is one when Io is at a positive declination and when the (earth-south threaded field intersection) angle is between 80° and 100°, and is zero at other times. The probability histogram for the phase of Io and the longitude of Jupiter is shown in Figure 10. Four major emission regions result. Three correspond to the predominantly observed emission regions and the fourth to the infrequently observed region. The fourth source, D, it is important to note, may be as active as the other three but as it occurs at a low frequency its observation is more difficult. There appears to be close but not perfect agreement between the four calculated and the four observed regions. This may relate to a non-dipole field configuration or to a different location of the Jovian dipole. The shaded areas in Figure 10 are observed radio burst probabilities greater than 30% whereas the ova. indicate probabilities close to 100%. These differences relate to the choice of the probability function of the earth-south threaded field intersection an-l .

Utilizing a centered dipole model, Figure 11 shows a histogram of the angle between the earth and the footpoint of the field line from Io. The north and south footpoint angles degenerate to the same quantity in this situation. Thus one may not choose either footpoint to be a more likely candidate for the emission region in this case. The magnetic declination of Io as a function of Io phase and the longitude of Jupiter is shown in Figure 12. Again a positive declination appears favorable for emission. Utilizing the criteria that the earth-south (or north) footpoint angle

is between 87° and 93° and that the Io magnetic declination is positive results in a probability of emission histogram shown in Figure 13. The size of the regions and the associated probabilities appear to be in good agreement with the observed probability distributions. Emission region A appears to be slightly displaced from its observed position.

An illustration of the sensitivity on Io phase is shown in Figure 3. The emission of radio bursts in this model occurs perpendicular to the footpoint field line. This is shown by the circular disk centered about the northern footpoint representing the plane of emission. As Io phase changes, this disk precesses about the Jovian magnetic axis and emission abruptly ceases. The sensitivity of emission on Jovian longitude is partly due to the shape of this emission disk but predominantly due to the magnetic declination of Io. Figure 12 shows the areas of positive magnetic declination. As can be seen there are broad areas, all of which correspond to the emission regions. The combination of these two effects results in the four emission sources.

The close agreement between the four calculated sources and the observed sources is a good indication that at least one of the footpoints of the field from Io and the magnetic declination of Io are related to the decametric radio bursts. This indicates that Io probably does not disturb the large-scale structure of the Jovian magnetic field and thus provides support for the non-conducting, non-magnetic hypothesis of Io's interaction with the Jovian magnetosphere. This hypothesis does not explain the large amount of energy observed in the Jovian decametric radio bursts.

Summary and Discussion

The location of the Io associated decametric radio bursts in an Io phase-Jovian longitude coordinate system were investigated assuming no large-scale influence of Io upon the Jovian magnetic field, represented by a Warwick off-center tilted dipole. The investigated locations where emission might be produced were near Io, or near the northern or southern footpoints of the magnetic field line from Io to the Jovian surface.

Assuming an emission probability of 1 when the (earth-south (or north) threaded field intersection) angle was between 87° and 93° and Io was at a positive declination and a probability of zero otherwise, a probability histogram was calculated. The probability of emission was calculated from 1961 through 1964 as a function of Io phase and Jupiter's longitude. Four emission regions were obtained that corresponded to the three prominent emission regions and to the infrequently observed one. The fits were better with a centered dipole model than with the Warwick offset model and both fits indicate that the source regions are likely associated with one of the footpoints of the field line from Io.

A model patterned after the solar wind-lunar interaction suggests the possibility that a similar mechanism may be occurring near Io leading to the stimulation of decametric radio emission. This model is consistent with the calculations represented in this paper.

ACKNOWLEDGEMENTS

We are appreciative of the discussion and help afforded to us by Joseph Alexander and Dr. Robert Stone of the NASA-Goddard Space Flight Center. We wish to further acknowledge Franklin Ottens for much of the programming involved in the computations.

REFERENCES

Behannon, K. W., J. Geophys. Res., 73, 7257 (1968).

Bigg, E. K., Nature, 203, 1008 (1964).

Burke, F. B. and Franklin, K. L., J. Geophys. Res., 60, 213 (1955).

Dulk, G. A.: Ph.D. Thesis, Astro-Geophysics Department, University of Colorado, Boulder, Colorado (1965).

Ellis, G. R. A., Radio Science, 69D, 1513 (1965).

Gledhill, J. A., Nature, 214, 155 (1967).

Goldreich, P. and Lynden-Bell, D., Astrophys. J., 156, 59 (1969).

Gulkis, S. and Carr, T. D., Science, 154, 257 (1966).

Marshall, L. and Libby, W. F., Nature, 124, 126 (1967).

Ness, N. F. and Schatten, K. H., J. Geophys. Res., 74, 6425 (1969).

Ness, N. F., NASA-GSFC preprint X-690-70-141 (1970).

Piddington, J. H. and Drake, J. F., Nature, 217, 935 (1968).

Smith, A. G., American Scientist, 57, 2, 177 (1969).

Warwick, J. W. Astrophys. J., 137, 41 (1963).

Warwick, J. W., Space Science Rev., 6, 841 (1967).

Zheleznyakov, V. V., Soviet Astron. 9, 617 (1965).

FIGURE CAPTIONS

Figure 1 Estimated joint probability distribution for decametric radio emission as a function of Jovian longitude, LCM, and the position of Io. Emission probability is labeled on the contour lines. The diagonal dashed lines illustrate the paths of the LCM-Io phase point on January 1, 1965. Observations from 1961 through 1964 were used in constructing this figure. (After Dulk, 1965).

Figure 2 Io and associated plasma disturbances arising as a result of super-Alfvenic magnetospheric-Io relative motion (top) or sub-Alfvénic relative motion (bottom).

Figure 3 Location of investigated decametric radio emission regions relative to Jupiter and Io. The region near Io and the regions near the north and south intersection points between the field line (shown) from Io and the surface of Jupiter were investigated. The emission was assumed to be emitted in a plane perpendicular to the field lines at one of these locations. The circular disk centered about the northern footpoint illustrates the emission region.

Figure 4 Computed average earth-Io field angle from 1961 through 1964 as a function of Io phase and Jupiter's longitude, system III (1957.0). Shading indicates regions near 90°. The Warwick tilted offset dipole model was used for the magnetic field as discussed.

Figure 5 Average earth-north threaded field intersection angle. Computed as in Figure 4.

Figure 6 Average earth-south threaded field intersection angle computed as in Figure 4.

Figure 7 Average north threaded field position angle to pole. Computed as in Figure 4.

Figure 8 Average south threaded field position angle to pole. Computed as in Figure 4.

Figure 9 Average magnetic declination of Io. Computed as in Figure 4.

Figure 10 Calculated probability histogram of decametric radio burst emission. Cross-hatched shading indicates observed joint probability distribution >30% and dotted shading indicates the location of the infrequently observed Jovian decametric radio source. See text for further discussion.

Figure 11 Average earth-north (or south) threaded field intersection angle computed for the centered dipole model. The shading indicates regions near 90°.

Figure 12 Average magnetic declination of Io for the centered dipole model.

Figure 13 Probability histogram as in Figure 10 but with a centered titled dipole field model.

YEAR	AUTHORS	MECHANISM
1963	Warwick	Field aligned radiation (Cerenkov emission)
1965	Zheleznyakov	Plasma waves in Jupiter's ionosphere
1965	Ellis	Cyclotron radiation from electron streams
1967	Gledhill	Io stimulated waves from a plasma discus
1968	Piddington and Drake	Io magnetized or highly conducting
1969	Goldreich and Lynden-Bell	Io unipolar conductor (moderate conductivity)
1970	Schatten and Ness	Io moonlike; radiation perpendicular to magnetic field connected to Io

TABLE 1

JOVIAN DECAMETRIC RADIO EMISSION THEORIES

Physical Characteristics of the Moon and Io

	Mass 10^{25} gm	Diameter Km	Density gm/cm^3
Moon	7.344	3476	3.34
Io	7.23	3240	4.06

Source: Blanco and McCuskey, 1961

TABLE II

PROBABILITY OF DECAMETRIC RADIO BURST EMISSION (OBSERVED)

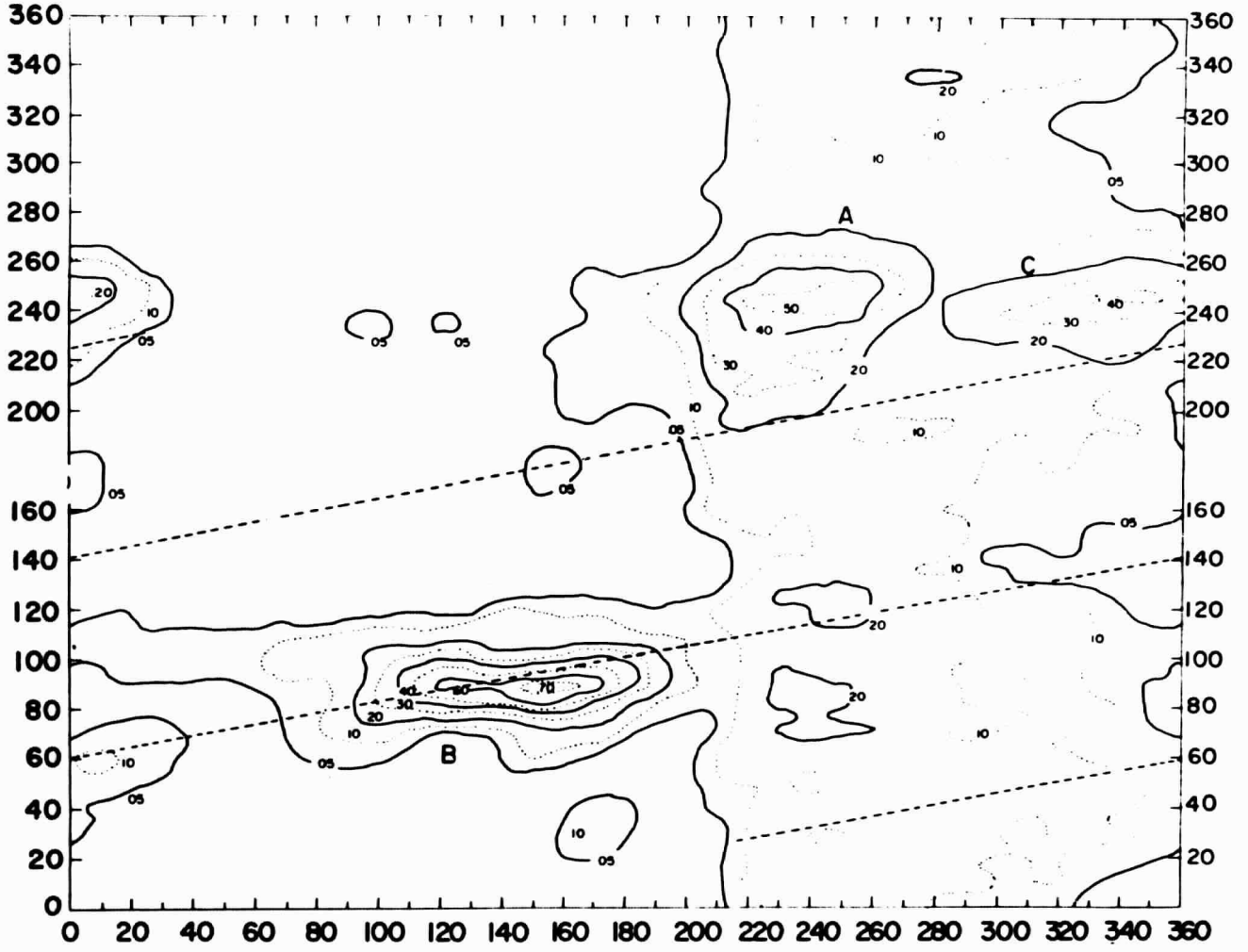

ϕ_{IO} (DEGREES)

LCM (DEGREES), SYSTEM III

FIGURE 1

SUPER-ALFVENIC RELATIVE MOTION

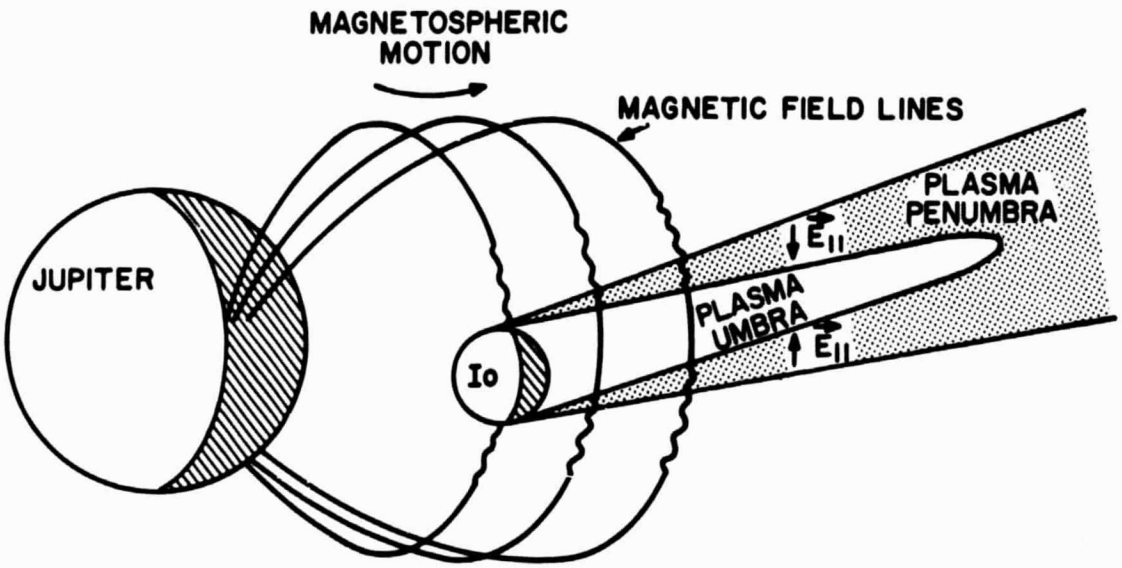

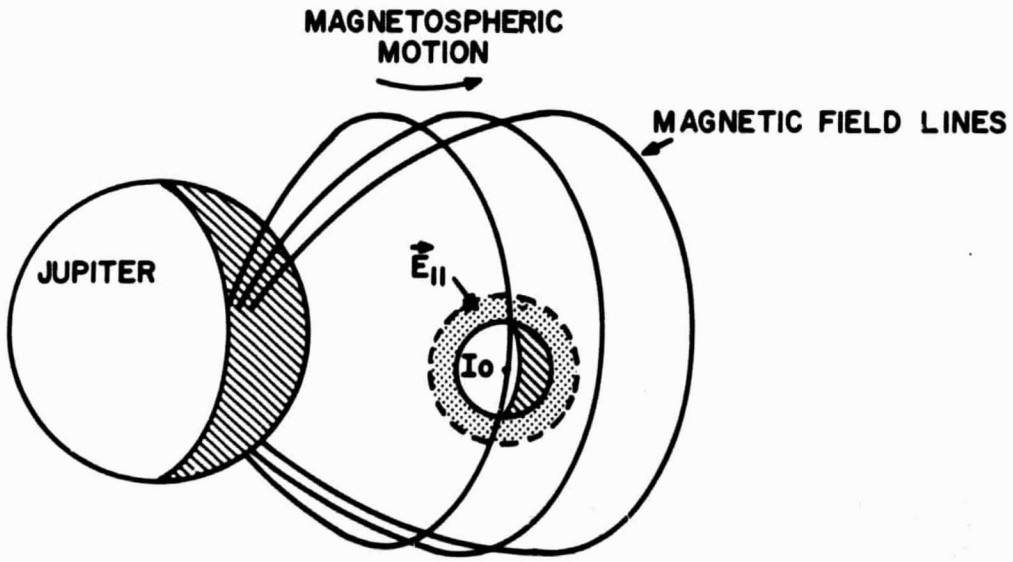

SUB-ALFVÉNIC RELATIVE MOTION

FIGURE 2

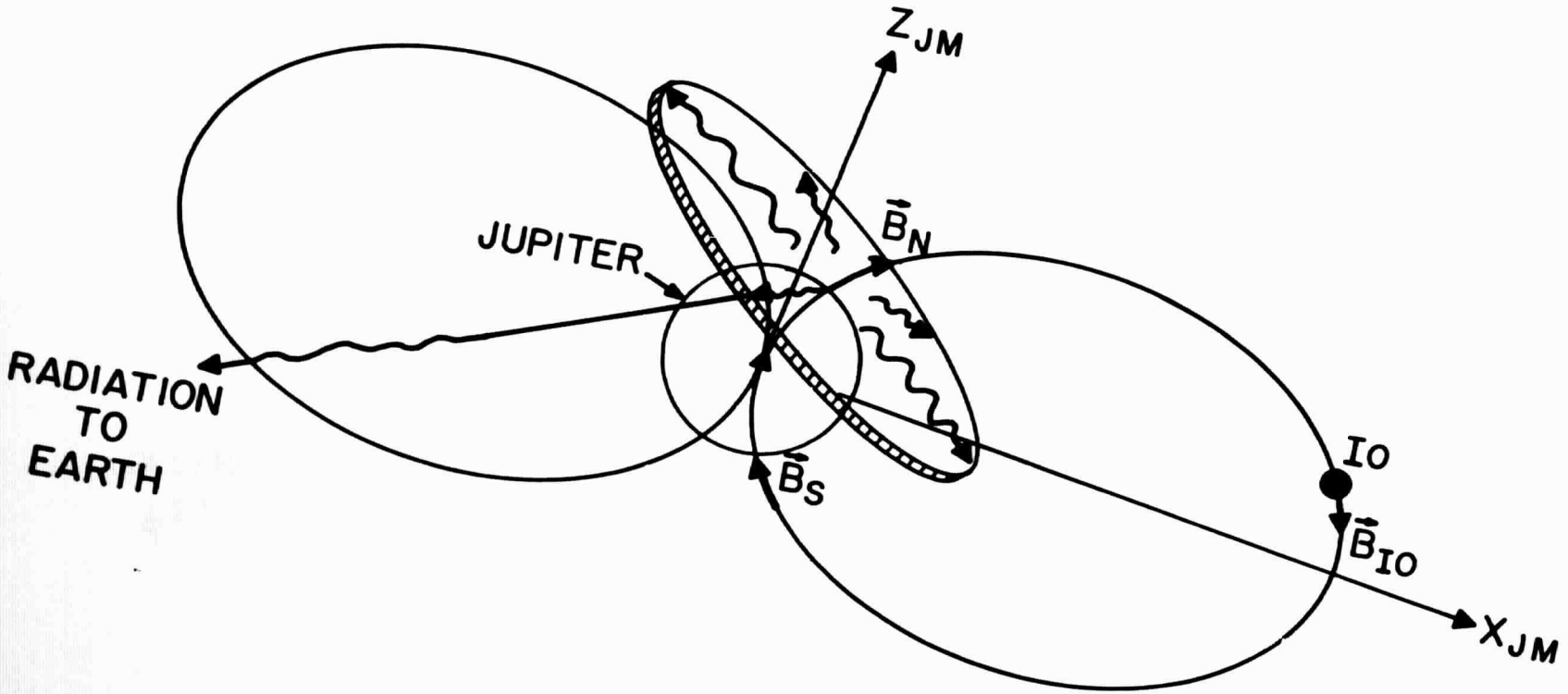

FIGURE 3

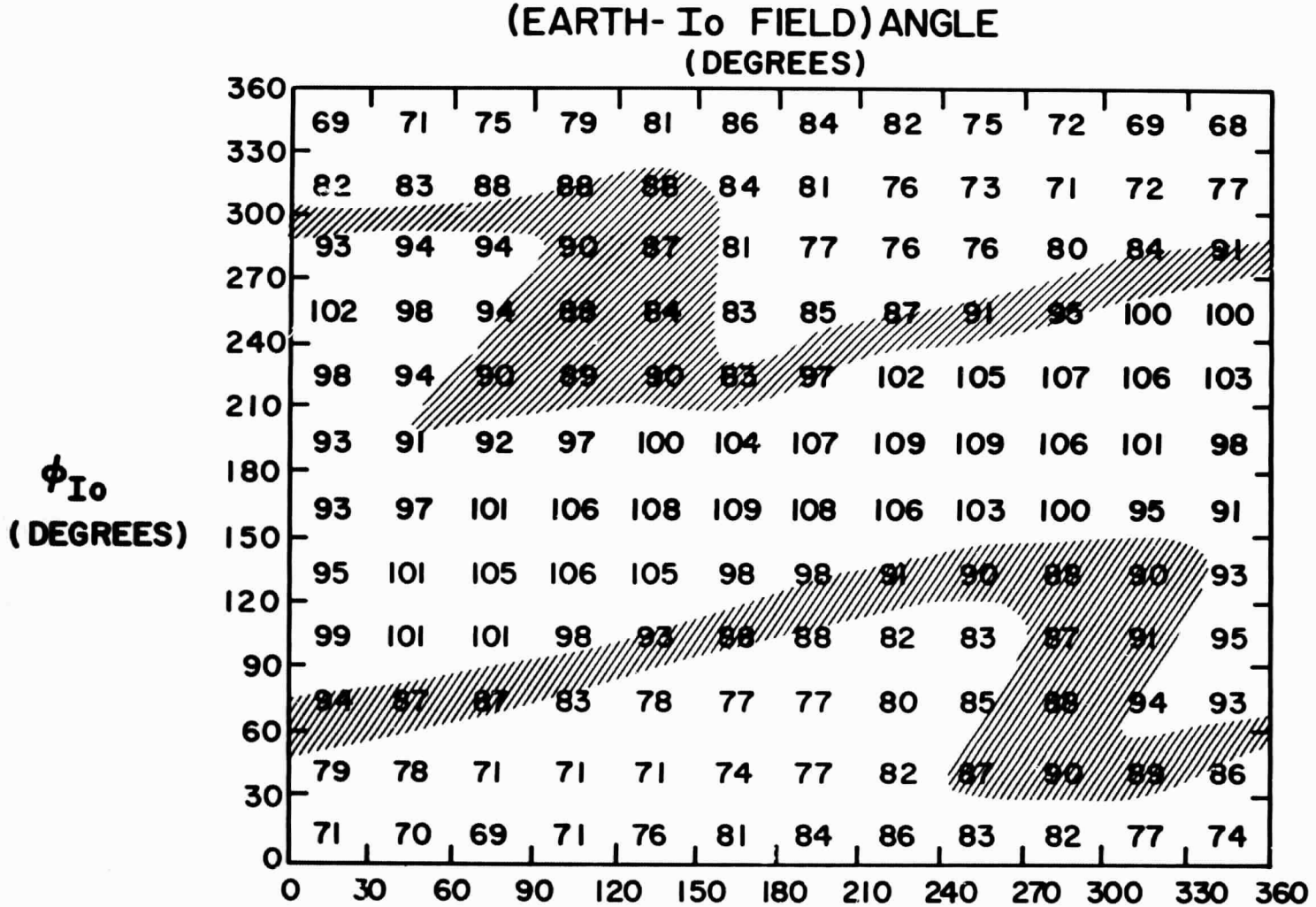

WARWICK TILTED OFF-CENTER DIPOLE MODEL

FIGURE 4

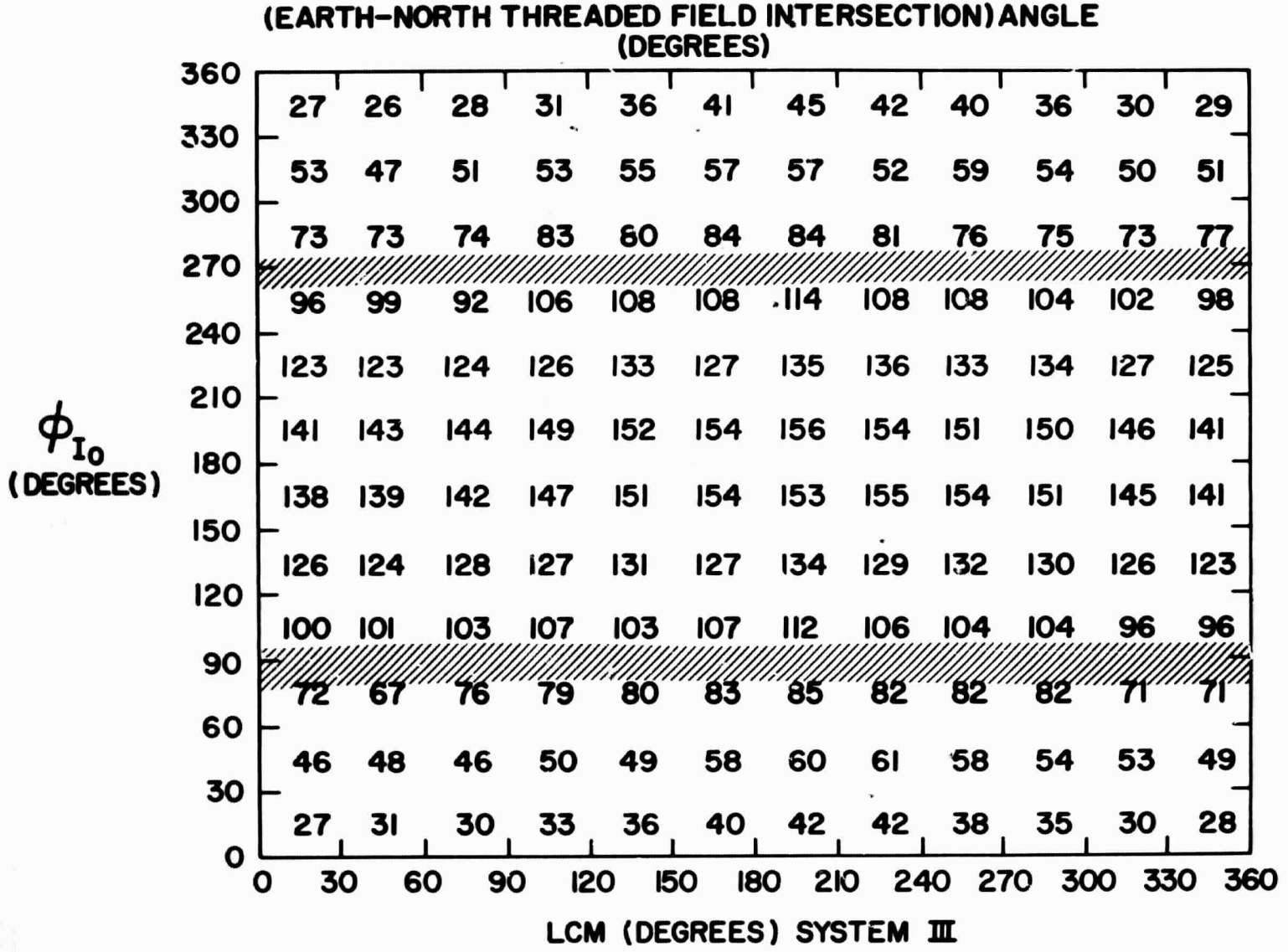

WARWICK TILTED OFF-CENTER DIPOLE MODEL

FIGURE 5

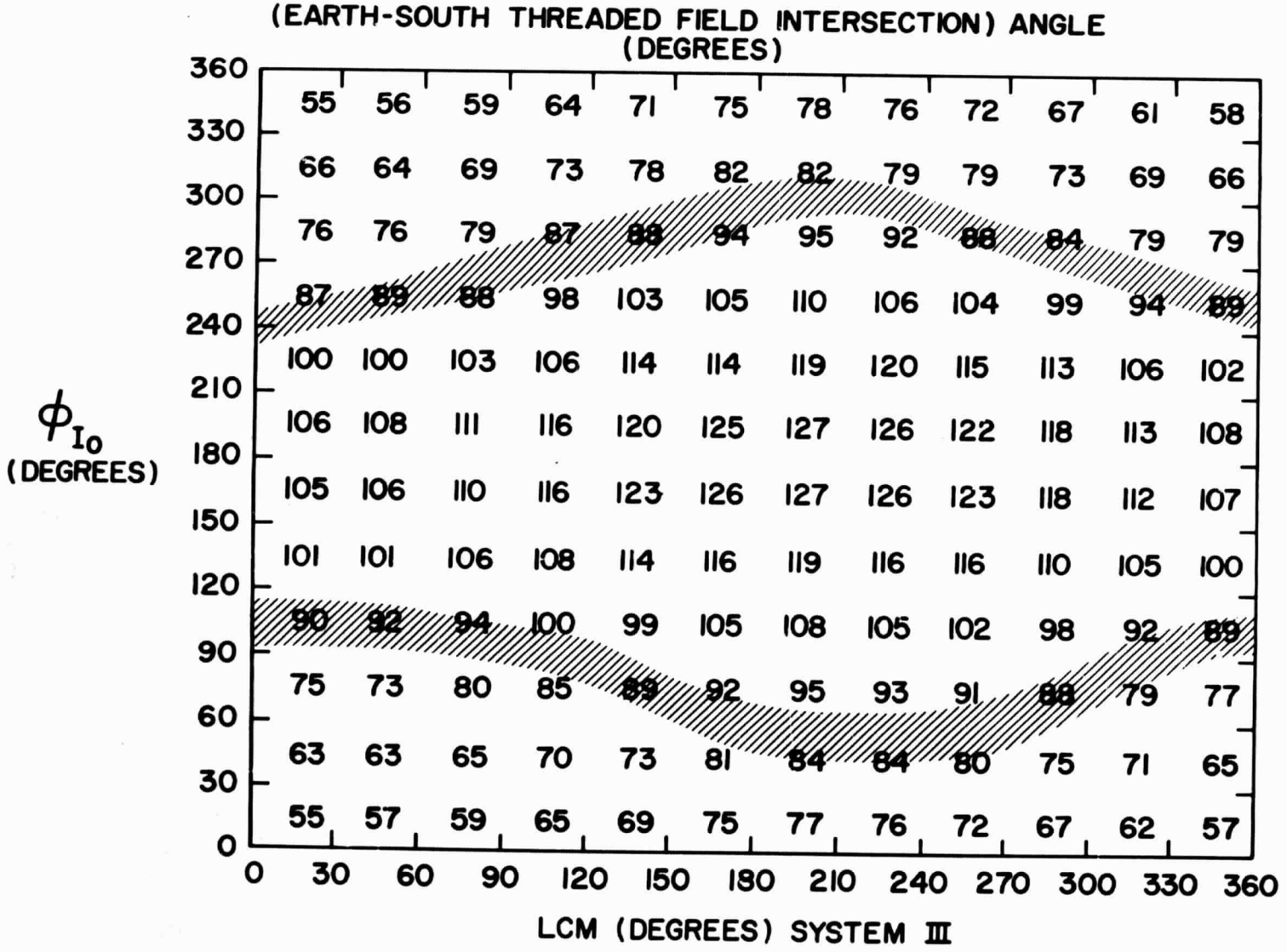

WARWICK TILTED OFF-CENTER DIPOLE MODEL

FIGURE 6

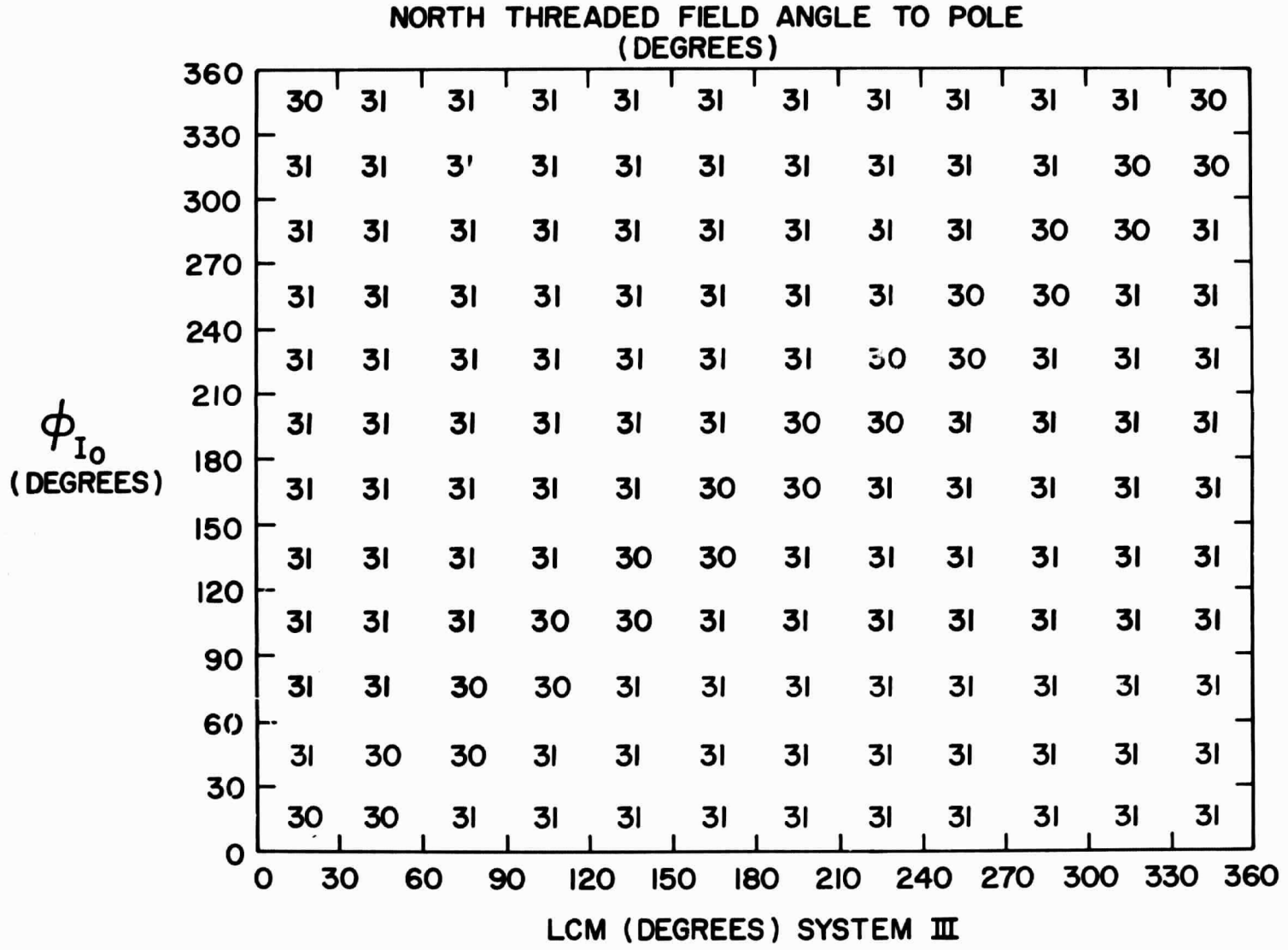

WARWICK TILTED OFF-CENTER DIPOLE MODEL

FIGURE 7

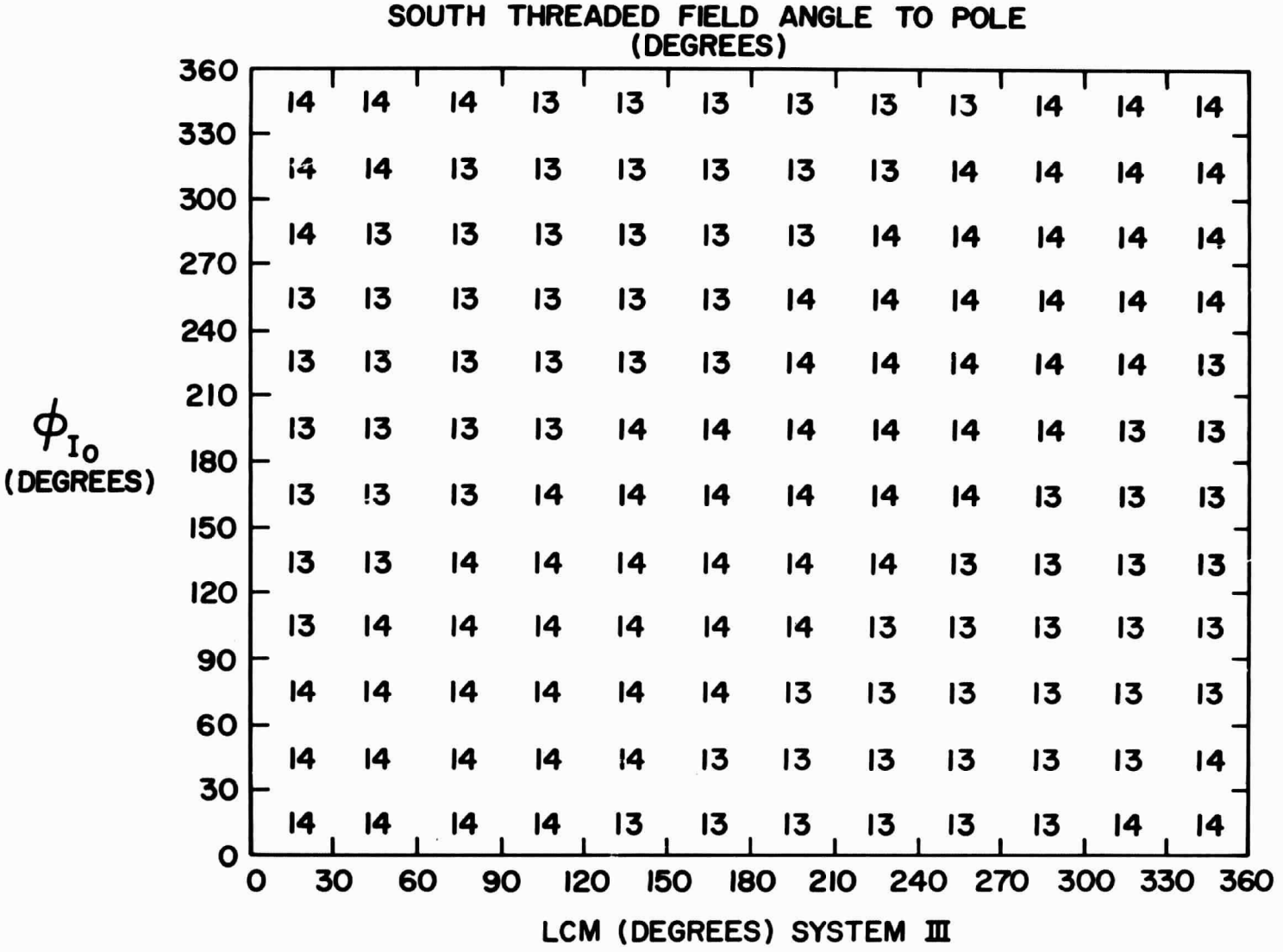

WARWICK TILTED OFF-CENTER DIPOLE MODEL

FIGURE 8

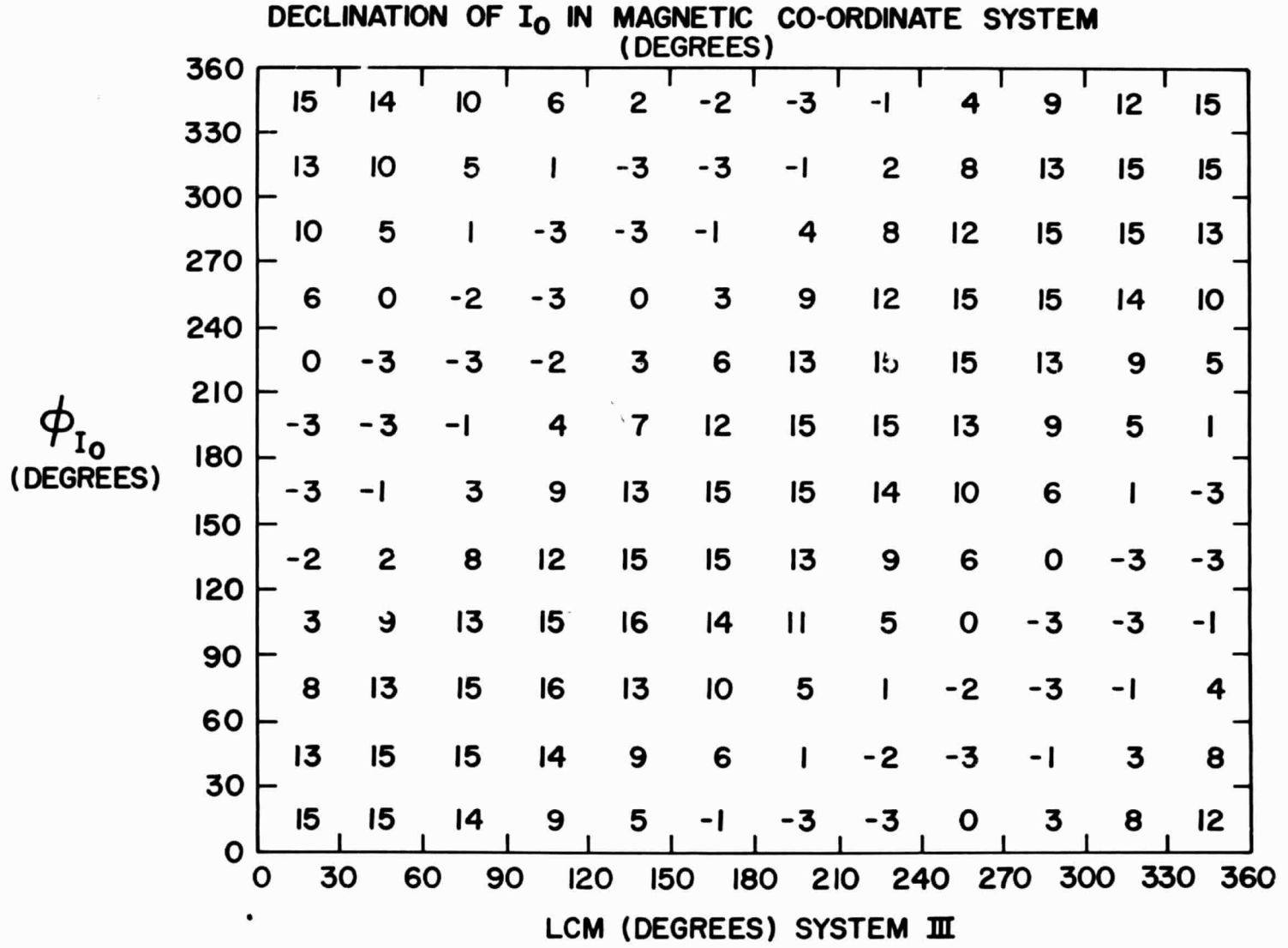

WARWICK TILTED OFF-CENTER DIPOLE MODEL

FIGURE 9

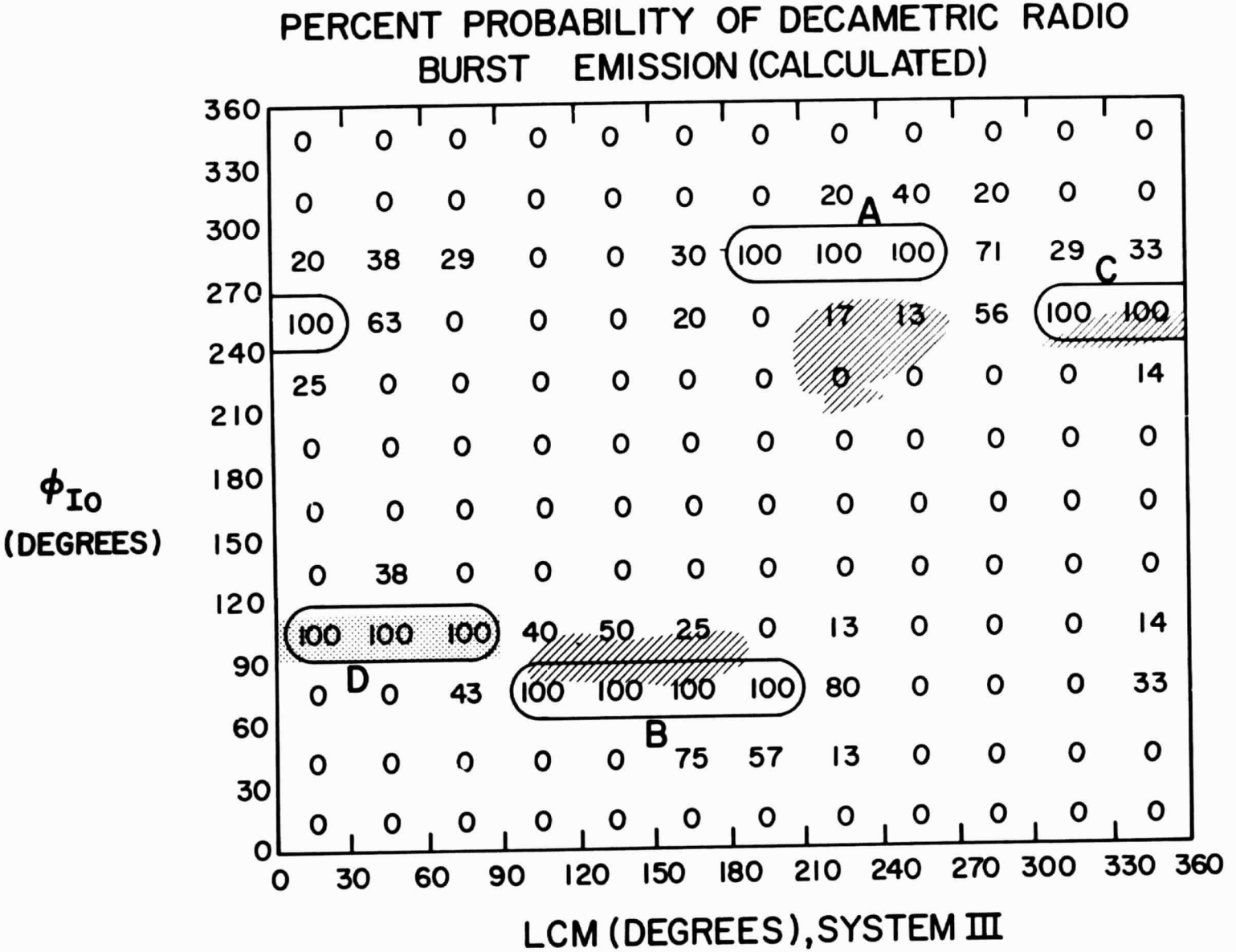
PERCENT PROBABILITY OF DECAMETRIC RADIO BURST EMISSION (CALCULATED)
ϕ_{Io} (DEGREES)
360
330
300
270
240
210
180
150
120
90
60
30
0
0 0 0 0 0 0 0 0 0 0 0 0
0 0 0 0 0 0 0 20 40 20 0 0
20 38 29 0 0 30 100 100 100 71 29 33
100 63 0 0 0 20 0 17 13 56 100 100
25 0 0 0 0 0 0 0 0 0 0 14
0 0 0 0 0 0 0 0 0 0 0 0
0 0 0 0 0 0 0 0 0 0 0 0
0 38 0 0 0 0 0 0 0 0 0 0
100 100 100 40 50 25 0 13 0 0 0 14
0 0 43 100 100 100 100 80 0 0 0 33
0 0 0 0 0 75 57 13 0 0 0 0
0 0 0 0 0 0 0 0 0 0 0 0
A
B
C
D
0 30 60 90 120 150 180 210 240 270 300 330 360
LCM (DEGREES), SYSTEM III
WARWICK TILTED OFFSET DIPOLE MODEL

FIGURE 10

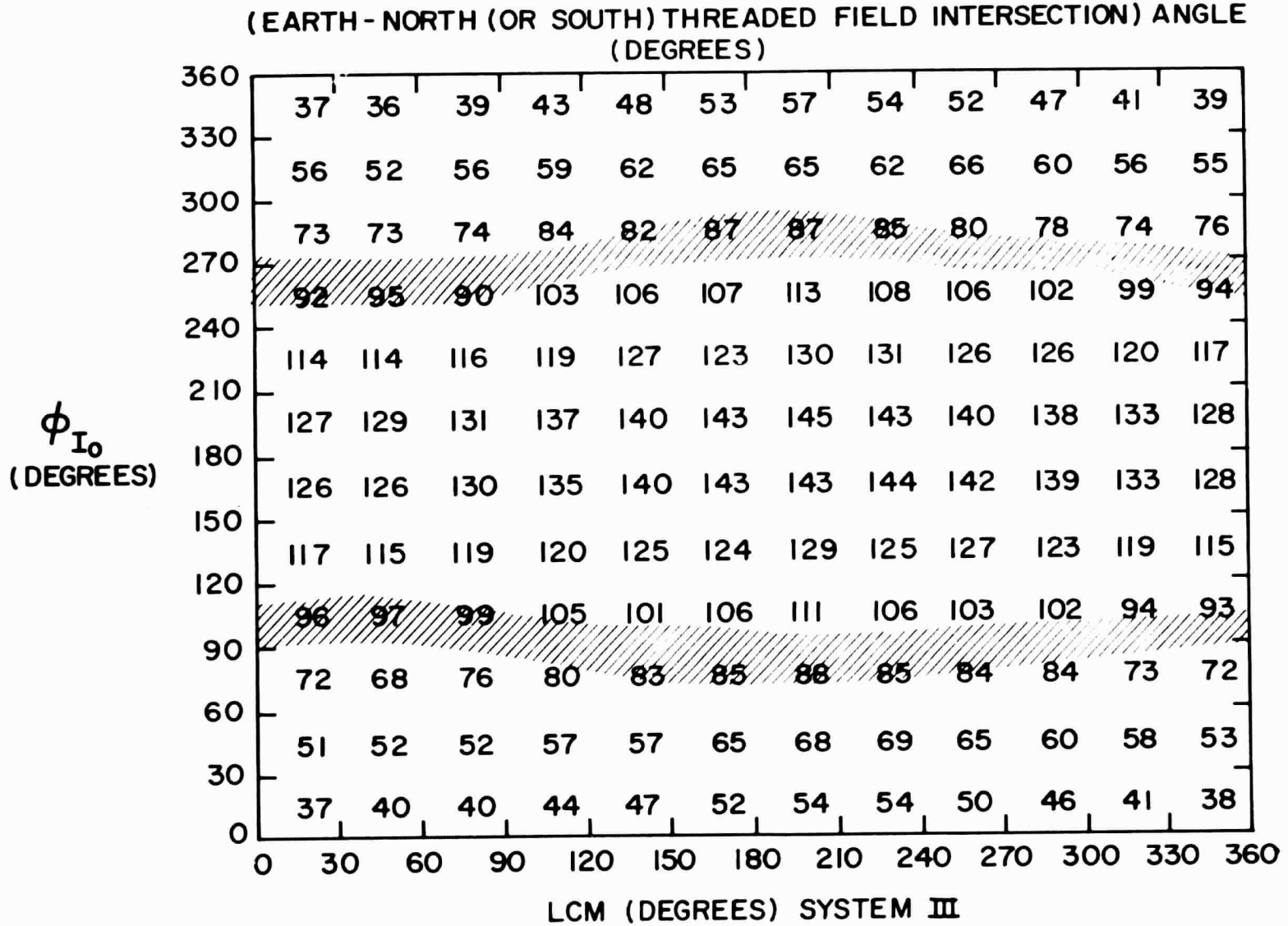

CENTERED TILTED DIPOLE MODEL

FIGURE 11

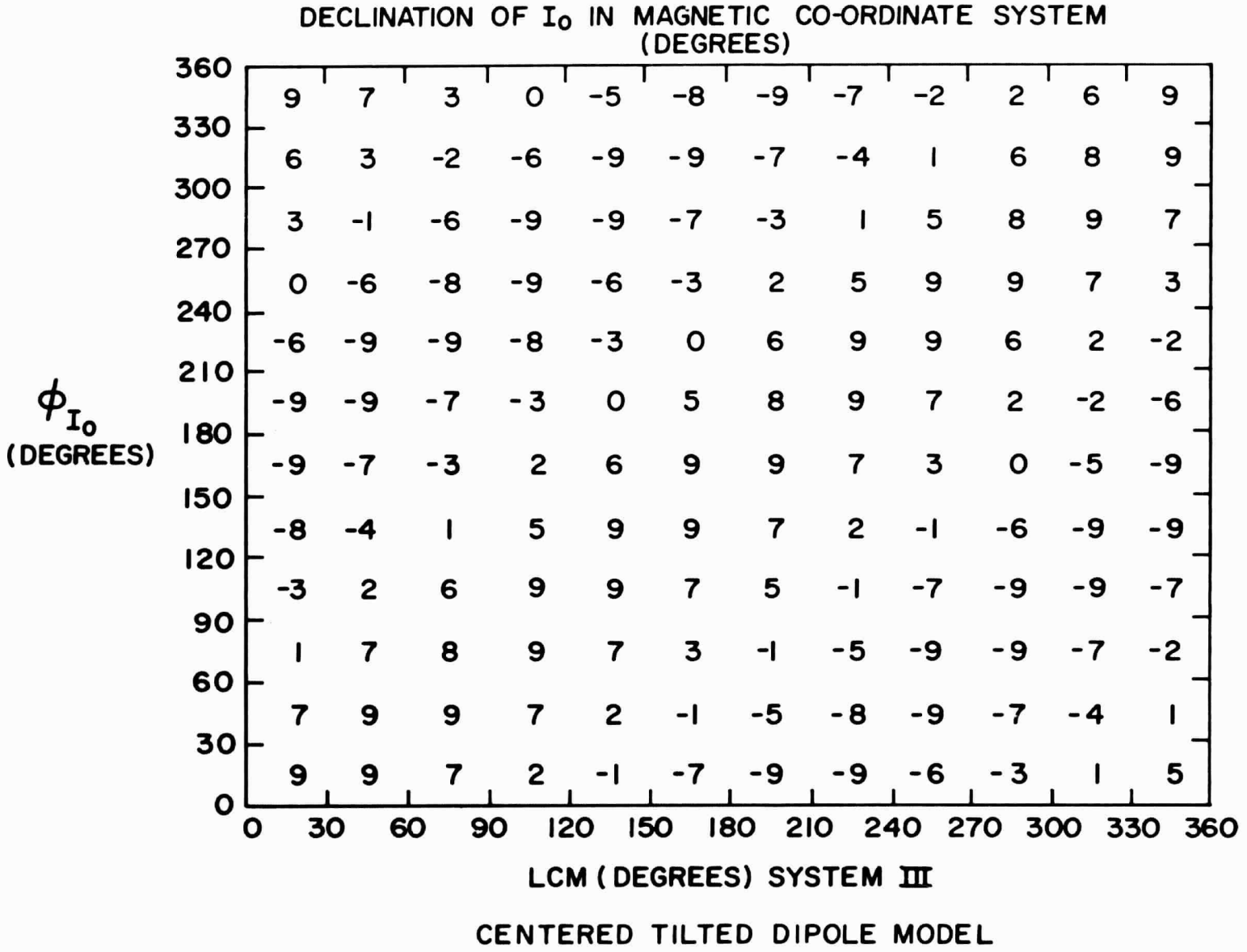
DECLINATION OF I_o IN MAGNETIC CO-ORDINATE SYSTEM
(DEGREES)
ϕ_{I_o}
(DEGREES)
360
330
300
270
240
210
180
150
120
90
60
30
0
9 7 3 0 -5 -8 -9 -7 -2 2 6 9
6 3 -2 -6 -9 -9 -7 -4 1 6 8 9
3 -1 -6 -9 -9 -7 -3 1 5 8 9 7
0 -6 -8 -9 -6 -3 2 5 9 9 7 3
-6 -9 -9 -8 -3 0 6 9 9 6 2 -2
-9 -9 -7 -3 0 5 8 9 7 2 -2 -6
-9 -7 -3 2 6 9 9 7 3 0 -5 -9
-8 -4 1 5 9 9 7 2 -1 -6 -9 -9
-3 2 6 9 9 7 5 -1 -7 -9 -9 -7
1 7 8 9 7 3 -1 -5 -9 -9 -7 -2
7 9 9 7 2 -1 -5 -8 -9 -7 -4 1
9 9 7 2 -1 -7 -9 -9 -6 -3 1 5
0 30 60 90 120 150 180 210 240 270 300 330 360
LCM (DEGREES) SYSTEM III
CENTERED TILTED DIPOLE MODEL

FIGURE 12

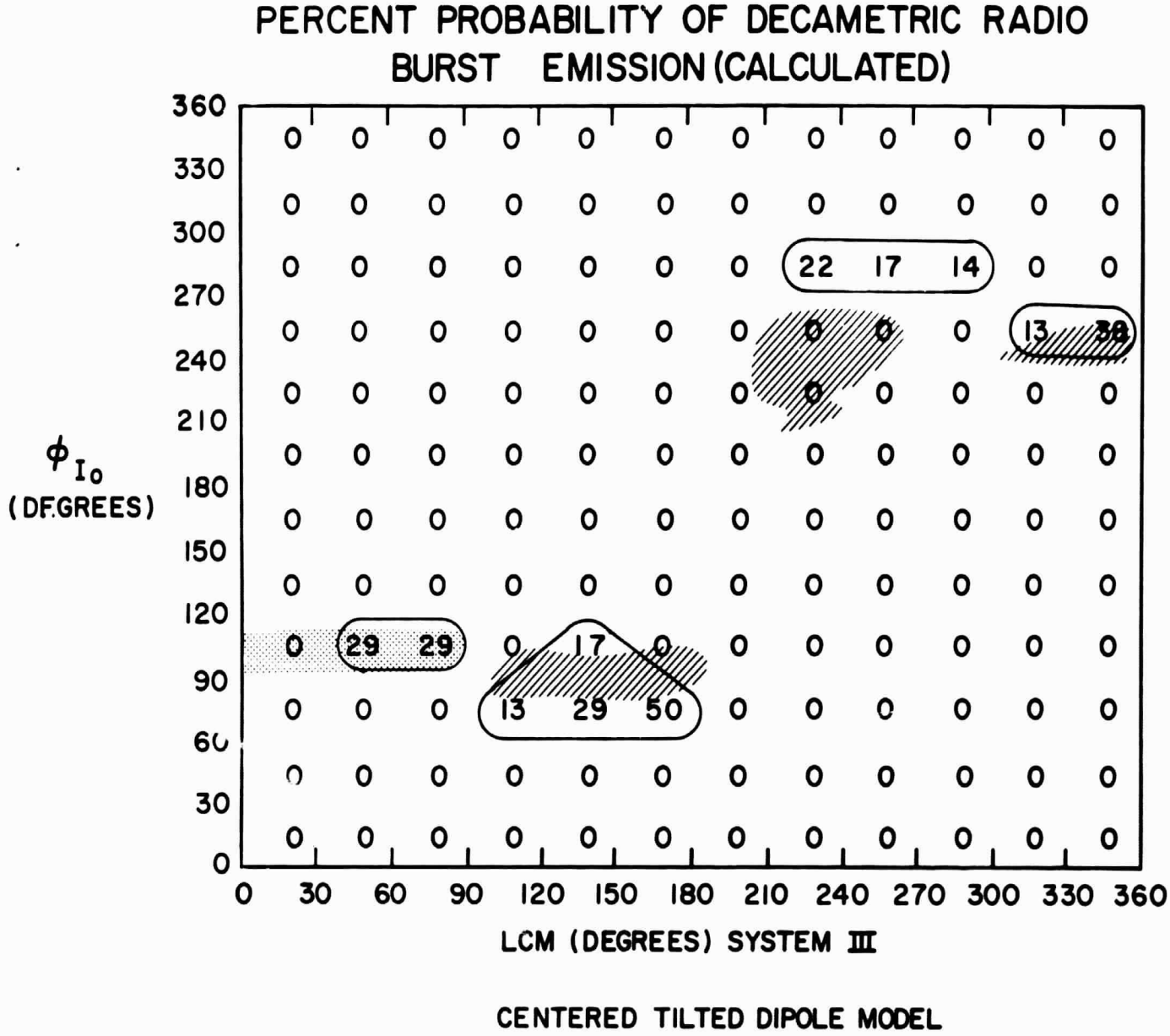
PERCENT PROBABILITY OF DECAMETRIC RADIO BURST EMISSION (CALCULATED)
ϕ_{I_o} (DEGREES)
360
330
300
270
240
210
180
150
120
90
60
30
0
0 30 60 90 120 150 180 210 240 270 300 330 360
LCM (DEGREES) SYSTEM III
CENTERED TILTED DIPOLE MODEL

FIGURE 13